Computational design of carbon nanotube electromechanical pressure sensors

Jian Wu,[1,2] Ji Zang,[2] Brian Larade,[3] Hong Guo,[3] X. G. Gong,[4] and Feng Liu[2,*]

[1]*Center for Advanced Study, Tsinghua University, Beijing 100084, People's Republic of China*
[2]*Department of Materials Science and Engineering, University of Utah, Salt Lake City, Utah 84112, USA*
[3]*Department of Physics, McGill University, Montreal, Canada PQ H3A 2T8*
[4]*Department of Physics, Fudan University, Shanghai 200433, People's Republic of China*

We investigate electronic transport properties of single-walled carbon nanotubes (SWNT's) under hydrostatic pressure, using first-principles quantum transport calculations aided by molecular-dynamics simulation and continuum mechanics analysis. We demonstrate a pressure-induced metal-to-semiconductor transition in armchair SWNT's, which provides a basis for designing nanoscale tunable pressure sensors.

Recent advances in computational algorithms and super-computers have brought us into a new era of computational modeling and simulation. Computation has emerged as an additional method for scientific research in parallel to experiment and theory, not only used for elucidating experiments but also as an effective method for designing new materials and devices prior to their existence. One example is the computational design of the super-hard material of boron nitride demonstrated by Cohen *et al.*[1,2]

So far, computational design has mostly focused on predicting new materials, using first-principles total-energy calculations. Here, we demonstrate an example of another repertoire of computational design to predict device structures, using first-principles quantum transport (QT) calculations.

The correlation between mechanical and electrical properties of carbon nanotubes has led to the exploration of nanotube-based electromechanical devices. For example, computations have shown that radial deformation can induce electrical transitions in single-walled carbon nanotubes (SWNT's).[3–6] However, in these earlier studies, the radial deformation is caused by artificially squashing the tube, a process that is difficult to quantify and control for designing devices. Here, we investigate the mechanical and electrical properties of SWNT's under hydrostatic pressure, using first-principles QT calculations aided by molecular dynamic (MD) simulations and continuum mechanics analysis. We demonstrate that hydrostatic pressure can induce radial deformation and hence electrical transition of SWNT, through a physical process that can be readily quantified and controlled. It provides a unique and promising basis for creating nanoscale tunable pressure sensors.

The transport properties of armchair SWNT's under different pressures, including the current-voltage (*I-V*) curves, are calculated using a newly developed formalism[7] that combines the Keldysh nonequilibrium Green's function (NEGF) (Refs. 8–10) with pseudopotential-based real-space density-functional theory (DFT).[7,11] The main advantages of this NEGF-DFT approach are: (i) a proper treatment of the *open*-boundary conditions for the device system as required for quantum transport under external bias potentials; (ii) an atomistic treatment of the electrodes; and (iii) a self-consistent calculation of the charge density via NEGF thereby incorporating the effects of both the *scattering* and *bound* states present in the system.

In order to carry out self-consistent DFT analysis of the nanotube systems under the nonequilibrium transport condition, we calculate the electron charge density matrix $\hat{\rho}$ via the NEGF (Refs. 8,9) $G^<$,

$$\hat{\rho} = -\frac{i}{2\pi} \int dE G^<(E), \qquad (1)$$

where $G^<$ is obtained by using the Keldysh equation, $G^< = G^R \Sigma^< G^A$. Here $G^{R/A}$ is the retarded/advanced Green's function of the device that we calculate by direct matrix inversion; $\Sigma^<$ is the self-energy representing injection of charge from the electrodes,[8–10] which is obtained from self-energies Σ^L and Σ^R arising from coupling to the left and right nanotube electrodes, respectively, and the Fermi distribution functions of these electrodes.[7] With the density matrix we carry out DFT interactions in the usual fashion until numerical convergence up to 10^{-3} eV. The bias potential enters the self-consistent real-space solution of the Hartree potential, its important effect is naturally included in the NEGF $G^<(E)$. We use a *s*, *p*, *d* real-space atomic basis set[7,11,12] in the DFT analysis, where atomic cores are treated by the standard nonlocal norm conserving pseudopotential scheme.[13]

After DFT self-consistency is reached, the *I-V* curve is obtained as[8]

$$I = \frac{2e}{h} \int_{\mu_{min}}^{\mu_{max}} dE (f_l - f_r) T(E, V_b), \qquad (2)$$

where μ_{min} (μ_{max}) is the smaller (larger) of the chemical potentials of the left and right reservoirs; $T(E, V_b)$ is the transmission coefficient at energy E and bias potential V_b,[8,10]

$$T(E, V_b) = 4 \operatorname{Tr}[\operatorname{Im}(\Sigma^R) G^R \operatorname{Im}(\Sigma^A) G^A]. \qquad (3)$$

It is emphasized that the functions inside the trace in Eq. (3) are all functions of bias potential V_b, as the current is calculated from a self-consistent analysis.

MD simulations were first performed to obtain the equilibrium structures (shapes) of nanotubes under hydrostatic pressure, which are used as input atomic structures for QT calculations. The pressure induces a series of mechanical shape transitions, as shown in Fig. 1 for a (10,10) armchair
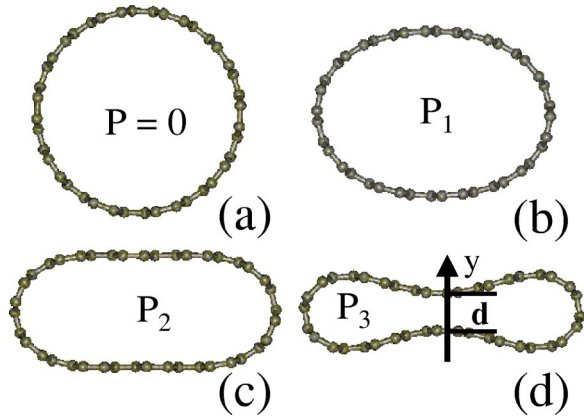
FIG. 1. MD simulated equilibrium shapes (cross sections) of a (10,10) SWNT at pressures of (a) 0, (b) 1.55, (c) 1.75, and (d) 2.2 GPa.

SWNT. It first transforms the tube from a circle to an ellipse at a critical transition pressure of $P_1 \sim 1.55$ GPa [Fig. 1(b)], and then from an ellipse to a dumbbell at a pressure of $P_2 \sim 1.75$ GPa [Fig. 1(c)].

Detailed analyses[14] show that the first shape transition from circle to ellipse is physically well defined, driven by a competition between compression and bending of the tube under pressure. Above a critical pressure (P_1), it becomes easier to bend (increasing the curvature) than to compress (reducing the perimeter) the tube. This leads to a spontaneous shape instability, transforming the tube from an isotropic circular shape to an anisotropic elliptical shape. Microscopically, it reflects the fact that it costs less energy to change bond angle than bond length, as evidenced from our MD simulations.[14,15] For this reason, the radial modulus (hardness) of the tube decreases by two orders of magnitude upon the first transition at a well-defined transition pressure.[14] Continuum mechanics calculations[14] show that the transition pressure P_1 scales with the tube radius inversely in a third-power law, $P_1 \approx 3D/R_0^3$, where R_0 is the original tube radius at zero pressure and D is flexural rigidity, a constant related to the modulus and Poisson ratio of the tube. Thus, the larger the tube, the sooner the transition. The dependence of P_1 on R_0 is shown in Fig. 2.

The second shape transition from ellipse to dumbbell is not physically well defined. It is actually caused by the geometric constraints, while the physical properties (such as hardness) of the tube are the same for the two different shapes (ellipse vs dumbbell). As the tube continues to shrink (reducing its cross-section area) under pressure, after the first transition it tends to reduce the overall curvature of the tube (maximizing bending) but maintain the length of its perimeter (minimizing compression).[15] (In contrast, before the first transition, the tube shrinks under pressure by reducing its radius, i.e., perimeter.) In doing so, it must eventually transform into a dumbbell shape, giving rise to the second shape transition. This is consistent with a mathematical theorem[16] that an enclosed boundary with fixed perimeter and constrained curvature will adopt a dumbbell (peanut) shape to have the minimum area. The second transition pressure (P_2) can be simply calculated as
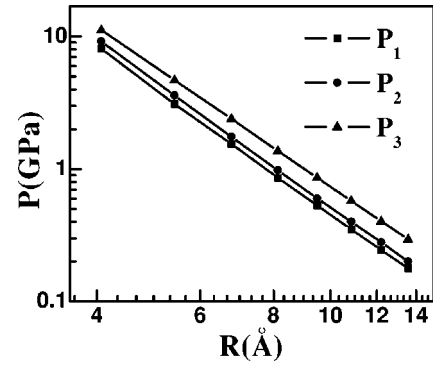

FIG. 2. The dependence of transition pressures on tube radius. The data points (squares, circles, and triangles) are results from MD simulations and lines are results from continuum mechanics calculation and variational geometry analysis. P_1 (squares): shape transition from circle to ellipse; P_2 (circles): shape transition from ellipse to dumbbell; P_3 (triangles): electrical transition from metal to semiconductor.

$$P_2 = P_1 - B_s \ln(A_2/A_1), \tag{4}$$

where A_2 and A_1 are the tube cross-sectional area at the transition pressures of P_2 and P_1, respectively. B_s is the radial modulus of the tube after the first transition, which approximately equals to $3D/R_0^3$.[17] Geometrically, A_2 corresponds to the point where the curvature becomes zero at the middle of the flattened area [normal to y direction, as shown in Fig. 1(c)]. Geometric analysis using the variational theorem shows that[17] the ratio of A_2 over A_1 turns out to be a universal constant, $A_2/A_1 \sim 0.819$, independent of tube radius. Thus, we have $P_2 \sim 1.2P_1$. This universal relation is further confirmed by MD simulations,[17] as shown in Fig. 2.

The pressure induced SWNT shape transition in turn induces an electrical transition.[3–6] Figure 3 shows QT calculations of the conductance versus energy at four different pressures, for the (10,10) SWNT. The equilibrium conductance is defined as $G = G_o T(E, V_b = 0)$. Here $G_o \equiv 2e^2/h$ is the conductance quantum. For the original armchair nanotubes at $P = 0$ there are two bands crossing Fermi energy E_f (Refs. 18,19) therefore $G = 2G_o$ at $E = E_f \equiv 0$. Experimentally, by making good electrical contact to SWNT, such a high con-
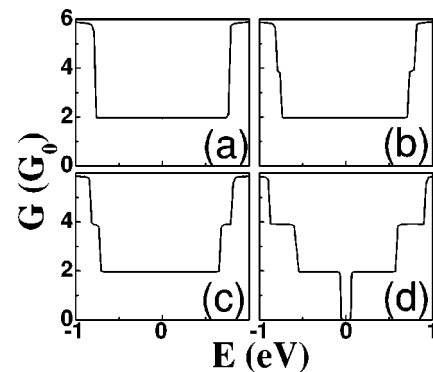

FIG. 3. Conductance (in units of $G_0 = 2e^2/h$) vs energy of a (10,10) SWNT at pressures of (a) 0, (b) 1.55, (c) 1.75, and (d) 2.2 GPa.
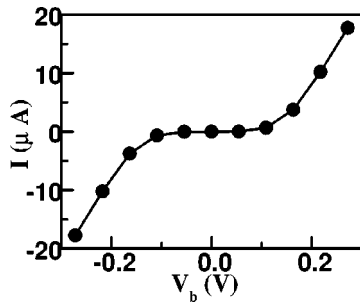
FIG. 4. The current-voltage (I-V) characteristics of the dumbbell (10,10) SWNT at 2.2 GPa, obtained from first-principles QT calculations.
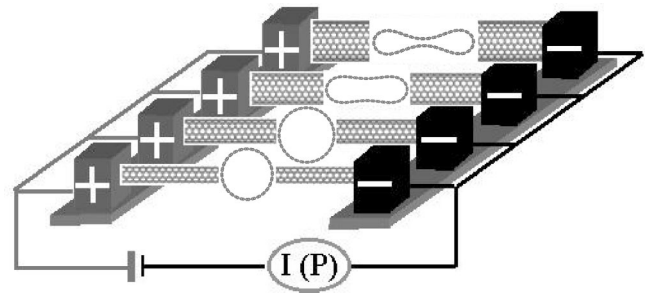

FIG. 5. The schematics showing a conceptual design of a tunable pressure sensor consisting of an array of armchair SWNT's of different sizes, sensing a broad range of pressures.

ductance has been recently obtained.[20] Away from $E = E_f$, $G(E)$ shows the familiar quantized steplike structure:[21] each time another electronic band of the SWNT is "cut" by the energy E, G increases by a unit of G_o. This steplike structure correlates perfectly with the band structure of the tube.

As pressure increases, the tube first transforms into an elliptical shape, breaking the original circular symmetry. The breaking symmetry lifts the degeneracy of the electronic energy bands. Consequently, the conductance curve displays extra steps at $4G_0$, as shown in Figs. 3(b)–3(d). The energy width of the extra steps increases with increasing pressure [from Fig. 3(b) to Fig. 3(d)], as the splitting of the degeneracy-lifted bands increases, due to larger structural deformation. As pressure further increases to 2.2 GPa, a noticeable qualitative change in conductance curve occurs. The conductance around Fermi energy drops by two orders of magnitude to zero, as shown in Fig. 3(d). This indicates that the tube undergoes a metal-to-semiconductor transition, which opens a band gap of ~ 0.12 eV. Figure 4 shows the I-V curve calculated by using Eq. (2) for the dumbbell tube at 2.2 GPa. It displays typical semiconductor I-V characteristics, in qualitative contrast to the linear behavior of the original metallic tube.

The metal-to-semiconductor transition for the dumbbell tube at 2.2 GPa is caused by a combined effect of the interaction between the two flattened areas [normal to y direction, as shown in Fig. 1(d)] of the dumbbell tube and a spontaneous breaking of mirror symmetry about y axis, which makes the two equivalent sublattices in the SWNT physically distinguishable.[6] The onset of transition can be estimated at where the minimum distance between the two flattened areas, d, is short enough so that atoms from the two flattened areas start to interact with each other (forming new bonds), as indicated in Fig. 1(d). The corresponding transition pressure (P_3) can be calculated, similar to P_2, as

$$P_3 = P_1 - B_s \ln(A_3/A_1), \qquad (5)$$

where A_3 is the tube cross-sectional area at P_3. By using the minimum distance d between the two flattened area of 2.6 Å, the cutoff length of C-C interaction, we can also numerically estimate the ratio of A_3 over A_1 for different tube size from MD simulations.[17] It is found that it varies slightly from 0.6 to 0.3 for armchair tubes ranging from (6,6) to (50,50). The dependence of P_3 on R_0 is shown in Fig. 2.

The unique mechanical and electrical response of SWNT's to external pressure provides a direct and effective method for designing nanoscale pressure sensors. Most promising, the onset pressure (P_3) for the metal-to-semiconductor transition depends on tube size, decreases monotonically with increasing tube radius, as shown in Fig. 2. This allows us to create tunable sensors detecting different ranges of pressures by using tubes of different sizes. For example, the critical transition pressure P_3 for a (6,6) tube is ~ 8.5 GPa, but it becomes only 0.003 GPa (30 atm) for a (100,100) tube. Therefore, it is possible to sense a wide range of pressures, e.g., from 30 to 10^5 atm, by using a combination of tubes of different radii, e.g., from (6,6) to (100,100). The fabrication of SWNT's of the size up to (50,50) has already been achieved.[22]

Figure 5 shows a proof-of-principle design of such a pressure sensor consisting of an array of armchair SWNT's of different sizes (radii) of (14,14), (16,16), (18,18), and (20,20). At a given pressure (~ 0.3 GPa), tubes will adopt different shapes depending on their sizes: the smaller tubes (14,14) remain circular; the medium tubes (16,16) become elliptical; and the larger tubes (18,18) and (20,20) change to dumbbell. Furthermore, among the dumbbell tubes, the largest one (20,20) will undergo the electrical transition becoming semiconducting. The combination of different shapes of tube, and hence the combination of the numbers of metallic versus semiconducting tube changes with pressure, as more tubes become semiconducting with increasing pressure. Thus, by connecting all the tubes into a circuit, the overall conductance for all the tubes effectively determines the external pressure. More interestingly, tunable pressure sensors for sensing different ranges of pressure can be made by using different combinations of the number and size of tubes.

MD simulations show that, at least up to a tube size of (20,20), the pressure induced shape transition, and hence the electrical transition is reversible upon releasing of pressure. Consequently, the pressure sensors made of these tubes can be used for many times with a long lifetime, given the excellent mechanical durability of carbon nanotubes. However, this reversibility may not sustain to even larger tubes, which are metastable in the original circular form, with a collapsed ground-state geometry.[23] For such tubes, however, one may still think of making a kind of one-time use pressure-sensible nanoscale alarming device, which cuts off the circuit (or power) at a particular pressure.

In conclusion, using first-principles quantum transport calculations aided by MD simulations and continuum mechanics analysis, we demonstrate a reversible pressure induced shape transition for armchair SWNT's, which in turn induces a reversible electrical transition from metal to semiconductor. Based on these findings, we propose a designing idea of nanoscale tunable electromechanical pressure sensors. Exploration of other forms of carbon nanotubes, such as those with different chiralities, multiwalled tubes, and bundle of tubes, will broaden the perspective of this potential application. Furthermore, the physical mechanism underlying the pressure induced shape transition is not limited either to carbon tubes or to nanoscale tubes. Therefore, the principles we demonstrate here can be extended to other kinds of nanotubes as well as to microtubes or macrotubes, with a broad range of potential applications.

---

*Electronic address: fliu@eng.utah.edu

[1] M.L. Cohen and A.Y. Liu, Science **245**, 841 (1989).

[2] E. Knittle, R.M. Wentzcovitch, R. Teanloz, and M.L. Cohen, Nature (London) **337**, 349 (1989).

[3] P.E. Lammert, P. Zhang, and V.H. Crespi, Phys. Rev. Lett. **84**, 2453 (2000).

[4] O. Glseren, T. Yildirim, S. Ciraci, and Ç. Kiliç, Phys. Rev. B **65**, 155410 (1997).

[5] Ç. Kiliç, S. Ciraci, O. Glseren, and T. Yildirim, Phys. Rev. B **62**, 16 345 (2000); O. Glseren, T. Yildirim, S. Ciraci, and Ç. Kiliç, *ibid.* **65**, 155410 (2002).

[6] J.Q. Lu, J. Wu, W.H. Duan, F. Liu, B.F. Zhu, and B.L. Gu, Phys. Rev. Lett. **90**, 156601 (2003).

[7] J. Taylor, H. Guo, and J. Wang, Phys. Rev. B **63**, R121104 (2001); **63**, 245407 (2001).

[8] A.P. Jauho, N.S. Wingreen, and Y. Meir, Phys. Rev. B **50**, 5528 (1994).

[9] B.G. Wang, J. Wang, and H. Guo, Phys. Rev. Lett. **82**, 398 (1999); J. Appl. Phys. **86**, 5094 (1999).

[10] S. Datta, *Electronic Transport in Mesoscopic Systems* (Cambridge University Press, New York, 1995).

[11] J. Taylor, Ph.D. thesis, McGill University, 2000.

[12] P. Ordejon, E. Archacho, and J.M. Soler, Phys. Rev. B **53**, R10441 (1996).

[13] D.R. Hamann, M. Schlüter, and C. Chiang, Phys. Rev. Lett. **43**, 1494 (1982).

[14] D.Y. Sun *et al.* (unpublished).

[15] MD simulations show that after the first transition, the bond length remains constant while the bond angle decreases with increasing pressure for both elliptical and dumbbell tubes.

[16] R. Howard and A. Treibergs, J. Math. **25**, 635 (1995).

[17] Ji Zang, A. Treibergs, Y. Han, and Feng Liu, Phys. Rev. Lett **92**, 105501 (2001).

[18] J.W. Mintmire, B.I. Dunlap, and C.T. White, Phys. Rev. Lett. **68**, 631 (1992).

[19] N. Hamada, S. Sawada, and A. Oshiyama, Phys. Rev. Lett. **68**, 1579 (1992).

[20] J. Kong, E. Yenilmez, T.W. Tombler, W. Kim, H.J. Dai, R.B. Laughlin, L. Liu, D.S. Jayanthi, and S.Y. Wu, Phys. Rev. Lett. **87**, 106801 (2001).

[21] L. Chico, M.P.L. Sancho, and M.C. Munoz, Phys. Rev. Lett. **81**, 1278 (1998).

[22] Y. Li, W. Kim, Y. Zhang, M. Rolandi, D. Wang, and H. Dai, J. Phys. Chem. B **105**, 11 424 (2001).

[23] N.G. Chopra, L.X. Benedict, V.H. Crespi, M.L. Cohen, S.G. Louie, and A. Zettle, Nature (London) **377**, 135 (1995).